A real-time nearshore wave and current prediction system

Richard Allard [a,*], James Dykes [a], Y.L. Hsu [a], James Kaihatu [a], Daniel Conley [b]

[a] *Naval Research Laboratory, Oceanography Division, Stennis Space Center, MS, United States*
[b] *NATO Undersea Research Centre, La Spezia, Italy*

Abstract

A nearshore wave, tide and current prediction system was demonstrated during the MREA04 Trial in the Portuguese coastal waters near Pinheiro da Cruz during the early spring of 2004. Daily forecasts of regional scale wave and tidal information and nearshore waves and currents were generated in DIOPS utilizing a suite of regional and nearshore models forced with data from meteorological and oceanographic production centers. A limited beach experiment was conducted with three Nortek current meters deployed in the surf zone and a video imagery system to generate 10-min time exposures used to identify the locations of wave breaking. In this study, Delft3D, a coastal hydrodynamic modeling system, capable of simulating hydrodynamic processes due to waves, tides, rivers, winds and coastal currents, is used to predict the nearshore wave and longshore currents near Pinheiro da Cruz. The nearshore bathymetry used in this study was based on LIDAR data collected in February 2000. Delft3D shows mixed results when compared with the measured wave height and nearshore currents. Improved Delft3D results can be achieved in the future if migrating sand bars can be measured and included in the modeling.
© 2007 Elsevier B.V. All rights reserved.

Keywords: Atmospheric forcing; Bathymetry; Longshore currents; Surf zone; Water level; Wave breaking

1. Introduction

A wave, tide and surf prediction system was implemented during the 2004 Maritime Rapid Environmental Assessment (MREA04) Trial for the Portuguese coastal waters southwest of Lisbon in late March through April 10, 2004. Real-time forecasts of nearshore wave, tide and surf conditions for beaches near Pinheiro da Cruz, Portugal, were generated aboard the NRV Alliance. Military critical operations may require a

nested modeling approach to produce reasonable estimates (and forecasts) of surf conditions for specific locations of interest. Inputs into these models include atmospheric forcing (winds), bathymetry, directional wave spectra and water levels. How good are the inputs into such models? Are the boundary conditions more important than the wind? This paper describes the DIOPS/Delft3D modeling approach, environmental inputs into these models and comparisons with in situ data. Although some of the input data were limited, we address how such a wave forecasting system can perform in an "operational" setting. The numerical results presented in this paper are from model hindcasts performed after the MREA04 Trial. The reasons for this are two-fold: (1) sensitivity studies were performed with

* Corresponding author.
  E-mail address: Allard@nrlssc.navy.mil (R. Allard).

a triple-nested wave model forced with winds from three different atmospheric models, and (2) computational resources available during MREA04 did not permit real-time high-resolution nearshore modeling with adequate temporal resolution to compare against in situ observations.

This paper is divided into seven sections. Section 2 provides some perspective on the MREA04 beach experiment and Rapid Environmental Assessment. Section 3 discusses the components of the Distributed Integrated Ocean Prediction System (DIOPS). In Section 4 we describe the nearshore modeling system Delft3D. Section 5 describes the observation and measurement systems used in this study. The results and analysis of these studies are detailed in Section 6. We discuss our findings in Section 7.

2. Background

The MREA04 Trial provided an opportunity to test and evaluate a beach environmental reconnaissance and monitoring system for amphibious warfare support. The study area near Pinheiro da Cruz was utilized during the NATO Linked Seas 2000 Exercise (Allard et al., 2000), an area used routinely for naval and amphibious training. The limited beach experiment was conducted by implementing high-resolution wave and surf models to depict the nearshore environment and deploy real-time data acquisition systems for situational analysis and bathymetry updates.

The beach experiment was conducted from April 2 to 11, 2004, near Pinheiro da Cruz. Instrumentation included video cameras and a high-resolution digital camera, three very shallow water Nortek current meters in the surf zone and a portable beach meteorological station. The systems contained data logging and real-time data transfer systems through satellite communications.

3. Modeling components

3.1. DIOPS

The Distributed Integrated Ocean Prediction System (DIOPS) is a wave, tide and surf prediction system (Allard et al., 2005) composed of the SWAN (acronym for Simulating Waves Nearshore) wave model; a relocatable tide model, PCTides; and the 1-D Navy Standard Surf Model (NSSM). SWAN is typically initialized by offshore directional wave spectra obtained from an operational production center. During MREA04, a triple-nested DIOPS SWAN forecast was

produced daily, with the innermost 100-m resolution nest providing boundary conditions to a very high resolution coupled wave/hydrodynamic modeling system called Delft3D. Details on Delft3D are discussed in Section 4.1.

During MREA04, DIOPS predictions were performed on a 400-MHz Sun Blade 100 UNIX workstation, while the PC-based Delft3D simulations were executed on a Dell Latitude C640 PC, with 1 GB of memory and a 2.1-GHz CPU. In the summer of 2004, DIOPS was ported to a windows based environment, allowing all calculations to be performed in the same (and faster) PC environment. In this study, while running on a Windows-based platform with a 3.1-GHz CPU, a 48-h prediction takes approximately 3 min for the tide model PCTIDES, 54 min for SWAN (host and 2 embedded nests, with the innermost nests utilizing PCTIDES water levels) and 2 h for Delft3D.

The Dynamic Information Architecture System (DIAS), developed by the Argonne National Laboratory, is a flexible, extensible, object-oriented framework for developing and maintaining complex simulations. DIAS is the DIOPS software object that allows these models to share needed information. The object-oriented DIOPS framework decomposes the maritime environment from the deep ocean to the shore into classes of software objects, each with its own spatially distributed sets of attributes, and with dynamic behaviors that are implemented by the appropriate ocean physics models. The models (e.g., SWAN and PCTides) communicate only with domain objects and never directly with each other. This makes it relatively easy to add or swap models without recoding. An atmosphere object provides the required meteorological forcing for all the DIOPS model components. Fig. 1 depicts the DIOPS model domain starting in deep water progressing to the surf zone. The user has the option of using the 1-D NSSM or Delft3D for surf prediction. A series of shell scripts processes output from SWAN and PCTides and generates input files for Delft3D calculations.

A DIOPS scenario consisting of SWAN and PCTides was set-up and loaded prior to the MREA04 Trial. Daily updates of wave spectra and meteorological forcing aboard the NRV Alliance were required to generate daily 48-h predictions of wave and water levels.

3.2. Meteorological models

Atmospheric model predictions available to MREA04 Trial participants were coordinated through different meteorological or defense institutions in Germany, Portugal, France and the United States. The
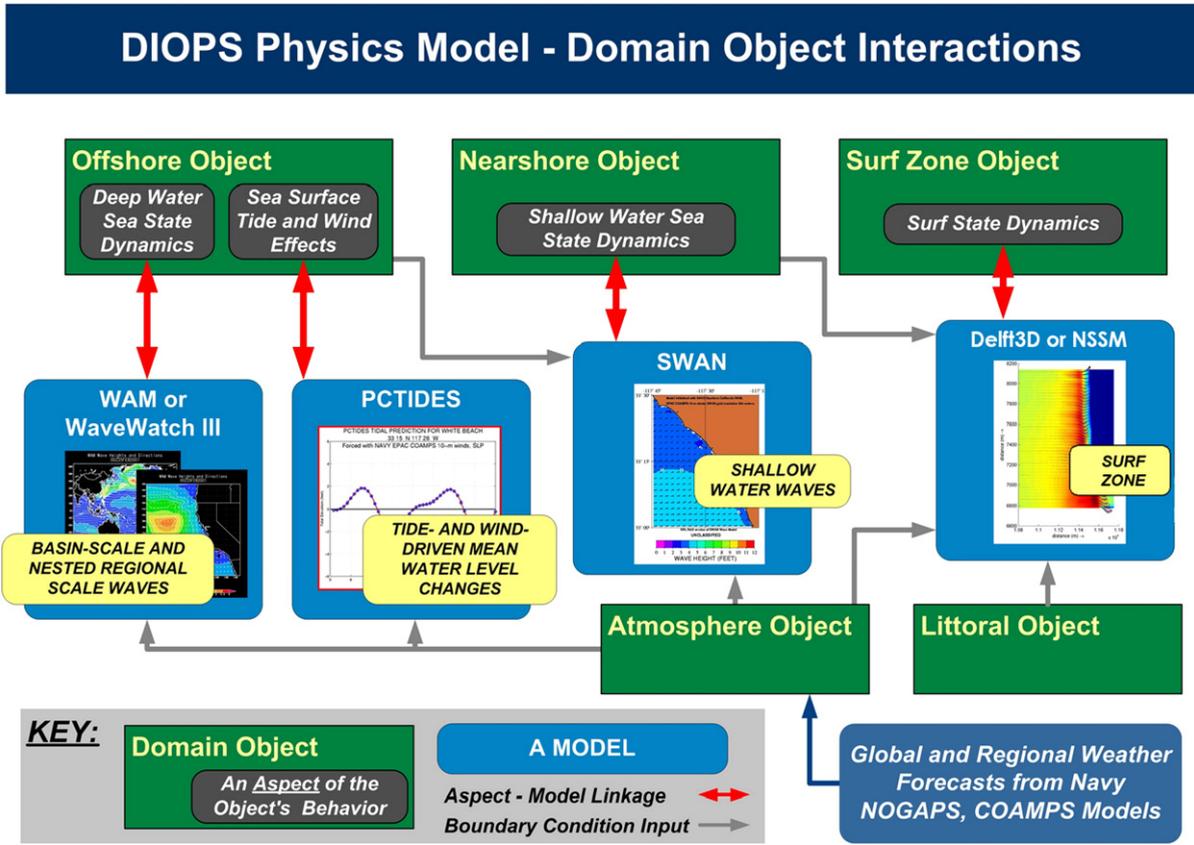
Fig. 1. Schematic diagram showing DIOPS model flow from deep water to the surf zone.

following section briefly describes the three models used in this study.

The U.S. Navy's Coupled Ocean/Atmosphere Mesoscale Prediction System (COAMPS®[1]) has been developed by the Naval Research Laboratory (Hodur, 1997) and is run operationally at the Fleet Numerical Meteorology and Oceanography Center (FNMOC) for numerous regions around the globe. COAMPS consists of an atmospheric data assimilation system comprising data quality control, analysis, initialization and non-hydrostatic forecast model components. The horizontal resolution of the COAMPS Europe application grid used in this study was 0.2°. Forecasts were available at six-hourly intervals out to 48 h. COAMPS Europe covers the entire Mediterranean originating at 15°W. COAMPS Europe was also used to drive the WAVE-WATCH III wave model (Tolman, 2002) that provided deepwater boundary conditions to the SWAN model

described in the next section. WAVEWATCH III is a third generation wave model developed at NOAA/NWS/NCEP.

For the present study, a particular set-up of the METEO FRANCE ALADIN (Aire Limitée Adaptation dynamique Développement InterNational) model (http://www.cnrm.meteo.fr/aladin) was used and provided by the French Service Hydrographique et Oceanographique de la Marine. The model domain extended from 11 to 8°W and from 36 to 40°N with a spatial resolution of 0.1° with forecast increments of 3 h available to 54 h twice daily.

The Deutscher Wetterdienst Lokal-Modell (DWD-LM) (http://www.dwd.de.en) covered the area from 34 to 42°N and 15 to 6°W. DWD-LM received boundary conditions from the DWD global model. The non-hydrostatic DWD-LM performs a continuous data assimilation based on an observational nudging scheme (Doms and Schattler, 1999). The LM is run operationally with a 7-km horizontal mesh and 35 vertical layers. The data provided during MREA04 were interpolated to a 0.05° horizontal resolution grid. DWD-LM contained

---

[1] COAMPS is a registered trademark of the Naval Research Laboratory.
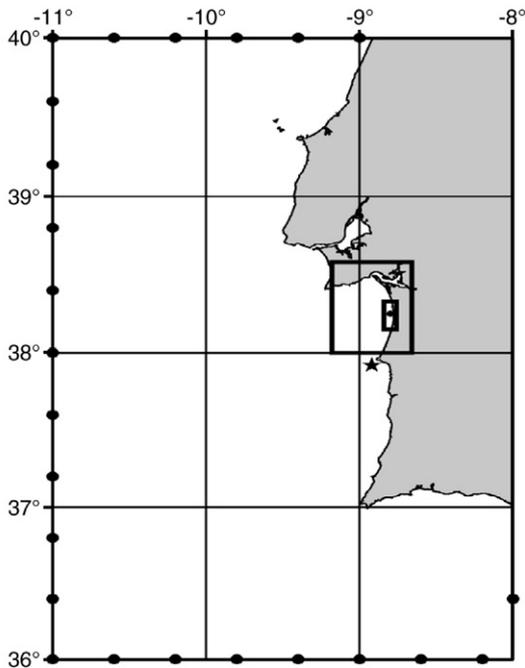
Fig. 2. Domain for triple-nest SWAN wave model computations performed during MREA04. Black circles indicate locations of WAVEWATCH III directional wave spectra applied as boundary conditions to SWAN host grid. Solid black rectangles indicate SWAN nests. Black star denotes locations of wave buoy near Sines.

the highest resolution of the three models examined in this study.

3.3. SWAN

SWAN (http://fluidmechanics.tudelft.nl/swan) is a third-generation, phased-averaged wave model (Booij et al., 1999; Ris et al., 1999) applicable at any scale, but most efficient when predicting wave conditions for small scales. It is capable of modeling coastal regions with shallow water, barrier islands, tidal flats, local winds and ambient currents. SWAN is based on the spectral action balance equation, treated in discrete form. Short-crested, random wave fields propagating simultaneously from widely varying directions can be accommodated. The SWAN model accounts for shoaling, refraction, wave generation due to wind, energy dissipation due to white-capping, bottom friction, depth-induced breaking and

non-linear wave–wave interactions (quadruplets and triads). Although the SWAN version used in these simulations (40.11) does not account for diffraction, version 40.41 has included diffraction in a phase-decoupled approximation.

A triple-nested SWAN wave forecast capability was established for the Portuguese coastal waters for MREA04; the nests are shown in Fig. 2. The host grid extended from 36 to 40°N and 11 to 8°W, with a grid resolution of 0.05°. All three nests contained 25 frequency bins ranging from 0.05 to 1.0 Hz, and directional bins ranging from 0 to 360° at 10° intervals. Boundary conditions of directional wave spectra were specified on the outer boundary of the SWAN host grid. Embedded nests with resolutions of 0.01° and 0.001° were contained within the host grid with boundary conditions provided via SWAN nesting files. Table 1 provides additional information about grid resolutions and settings used for these simulations. The inner nest of SWAN utilized water levels from PCTides (see Section 3.4) to adjust the water depths hourly.

The NATO Undersea Research Centre provided bathymetry for the outer two SWAN grids at resolutions of 6 and 12 s. The innermost SWAN nest covered an 18-km section of the beach area centered near Pinheiro da Cruz. The bathymetry for this 100-m resolution nest was based in part on the SHOALS (acronym for Scanning Hydrographic Operational Airborne LIDAR Survey) hydrographic data collected during the Linked Seas 2000 NATO Exercise. SHOALS was deployed on a Twin Otter aircraft in April 2000 over a two-day period to collect bathymetry for a 16-km section of coastline ranging from depths of 14 m above the low water line to depths of 22 m (Lillycrop et al., 2000).

The southwest coast of Portugal is predominantly affected by waves propagating from the northwest and west, with occasional motion from the southwest. Buoy statistics from the Sines buoy (http://www.hidrografico. pt/wwwbd/Boias/BoiasUltimoRegisto.asp) used in this study indicate a predominant wave direction from the northwest 60% of the time for the one-year period ending April 1, 2005, based on more than 30,000 hourly observations. The Pinheiro da Cruz beach is a sandy-cliff stretch (Pires-Silva et al., 2002) nearly centered in a soft cell coast (approximately 60 km in length) bounded by the Sado Estuary to the north and Sines Harbor to the

Table 1
Information about SWAN model configuration used during MREA04

	No. of X	No. of Y	LONGW	LONGE	LATS	LATN	RES	No. of direction	No. of frequency	BC	Timestep	
Grid A	61	81	349	352	36	40	0.05	36	24	WW3	15 min	NON
Grid B	52	59	350.82	351.33	38	38.58	0.01	36	24	Grid A nest	15 min	NON
Grid C	81	181	351.16	351.24	38.15	38.33	0.001	36	24	Grid B nest	3-hourly	STAT
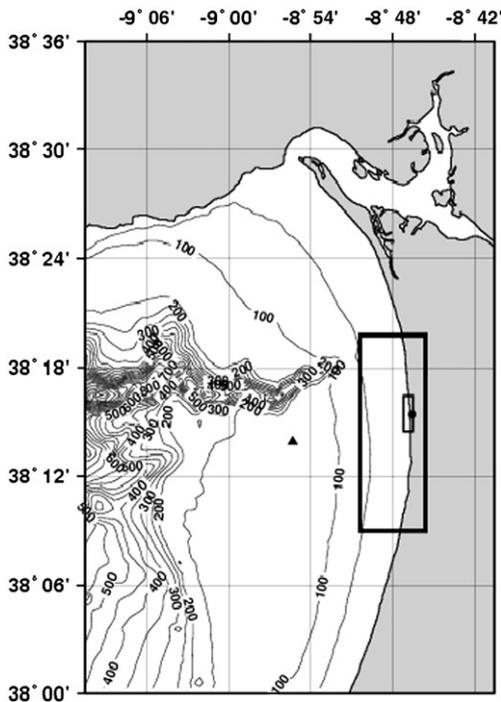
Fig. 3. Bathymetry near Pinheiro da Cruz, isobaths displayed at 50-m intervals. Circle near coast shows beach location; triangle denotes location of Meteo buoy. Black outer rectangle denotes SWAN inner nest (GRID C). Inner rectangle denotes Delft3D WAVE grid.

south. The bathymetry (Fig. 3) is fairly regular with contours paralleling the coast with the exception of the Setubal Canyon which terminates approximately 10 km northwest of Pinheiro da Cruz, the location of which is indicated by the black circle on the coastline in Fig. 3. During events with strong northerly to north–north-westerly winds, the region is sheltered from higher wave heights due to the short fetch.

The SWAN host was forced with boundary conditions from the 27-km Europe wave model WAVEWATCH III provided by the FNMOC. Directional wave spectra were provided via a METCAST server for the locations specified in Fig. 2 throughout the MREA04 Trial. WAVEWATCH III data were not available during the 00 GMT (Greenwich Mean Time) forecast cycles on March 30 and April 8, 2004. Missing fields were replaced with forecast data from the previous watch cycle. WAVE-WATCH III is forced with winds from the 27-km COAMPS Europe model runs.

3.4. PCTides

PCTides is a globally re-locatable tide/surge forecast system (Preller et al., 2002) consisting of three primary

components: (1) a grid generator that utilizes the Naval Research Laboratory's DBDB2 global bathymetry database and additional higher resolution regional databases; (2) a global tidal model, the Finite Element Solutions 99 (FES99) which is used to provide tidal conditions on open boundaries; and (3) a two-dimensional barotropic ocean model that produces predictions of water level
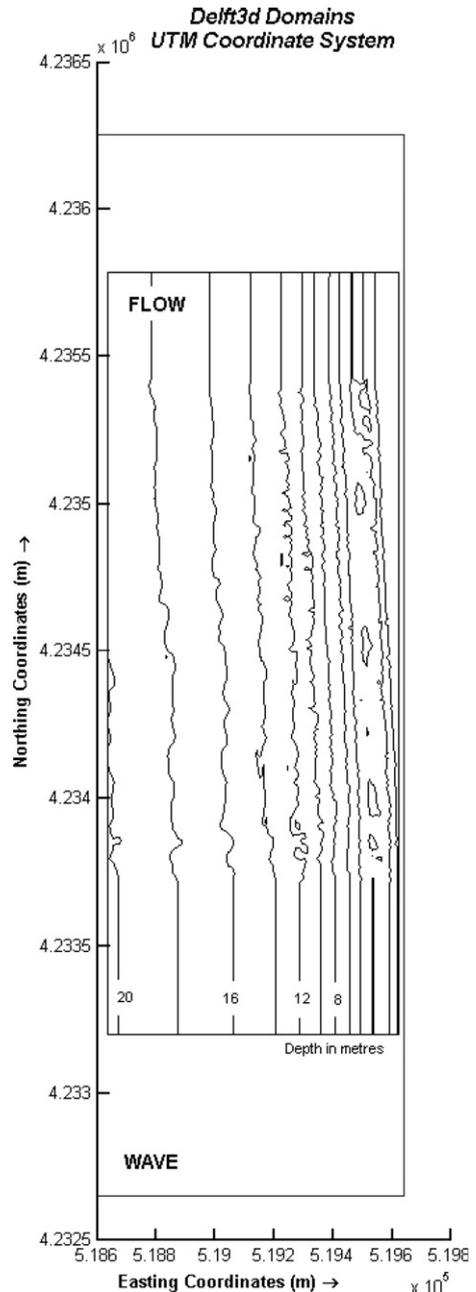
Fig. 4. Domains for WAVE denoted by large rectangle and FLOW denoted by visible bathymetry, whose depth values in meters are indicated by the color bar.

and depth-averaged currents. Options include the ability to assimilate International Hydrographic Office (IHO) tidal station data, wetting and drying and a surge capability that utilizes wind forcing and sea level pressure from operational meteorological models.

During MREA04, PCTides 48-h forecasts of water levels were provided daily for a grid encompassing the area from 34 to 40°N and 12 to 5°W with a resolution of 0.05° (PCTides can be run on either a Lambert Conformal or spherical grid). Tidal constituents for the M2, S2, N2, K2, K1, O1, P1, Q1 and 2N2 tides were extracted from the Finite Element Solutions 99 (Lefevre et al., 2002). DWD-LM winds and sea level pressure were used in the daily DIOPS run stream. The output was fed to the inner nest of SWAN to adjust bathymetry at hourly intervals. A total of 28 IHO stations were assimilated into the PCTides model solutions.

4. Near shore modeling system

4.1. Modeling description

The Delft3D system, developed by Delft Hydraulics (http://www.wldelft.nl), is a complete coastal hydrodynamic modeling system, capable of simulating hydrodynamic processes due to waves, tides, rivers, winds and coastal currents; the present application of the model is focused on nearshore hydrodynamics forced by breaking waves. The model can be run in rectangular (equidistant or stretched) or curvilinear coordinates; all necessary grid generation software for creating curvilinear grids is included with the Delft3D package.

The Delft3D system uses two modules for simulating nearshore wave-induced hydrodynamic processes. The WAVE module uses the SWAN model for propagation and generation of waves. Hydrodynamics are simulated with the FLOW module (WL Delft Hydraulics, 2001), which uses the three-dimensional hydrostatic shallow water Navier–Stokes equations with the discretization scheme of Stelling and Van Kester (1994). Forcing for wave-induced flow is derived from radiation stresses with both wave and roller contributions (Reniers et al., 2002; Roelvink, 2003). The model can be run with both one-way forcing or with feedback between the two modules. Although a highly flexible tool for various applications small and large, this component of the nearshore modeling system was tailored specifically for a domain that would extend from the shoreline to about
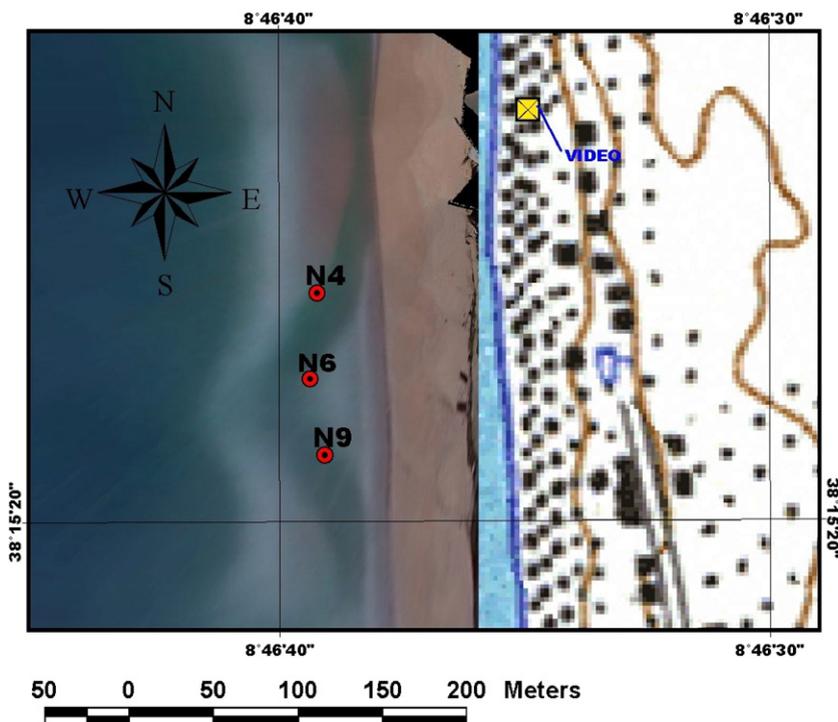
Fig. 5. Location of surf sensors at Pinheiro da Cruz. Sensors are overlain on rectified time exposed image of the surf zone created at low tide on April 7. The light areas in the image represent regions of persistent wave breaking and indicate the bar locations. Model results are compared primarily with the measurements collected from the Nortek velocimeter N6.

1 km seaward (Dykes et al., 2003). Morris (2001) first implemented and evaluated Delft3D with this specific application in mind.

Originally the NSSM provided surf conditions for a one-dimensional beach profile across the shore. Given accurate inputs from the host SWAN model, predictions from this model were sufficiently accurate provided there was minimal depth variability along the shore. However, when sufficient variability in water depths exists with bars and bar breaks, the one-dimensional predictions cannot account for currents due to the resulting variable longshore pressure gradient forces. Additionally, the NSSM can be considered a highly constrained model, in the sense that wave breaking and dissipation drives only the longshore current, with no ability to generate cross-shore flows like rip currents.

In this exercise, we used the Delft3D WAVE and two-dimensional FLOW modules. WAVE uses the SWAN
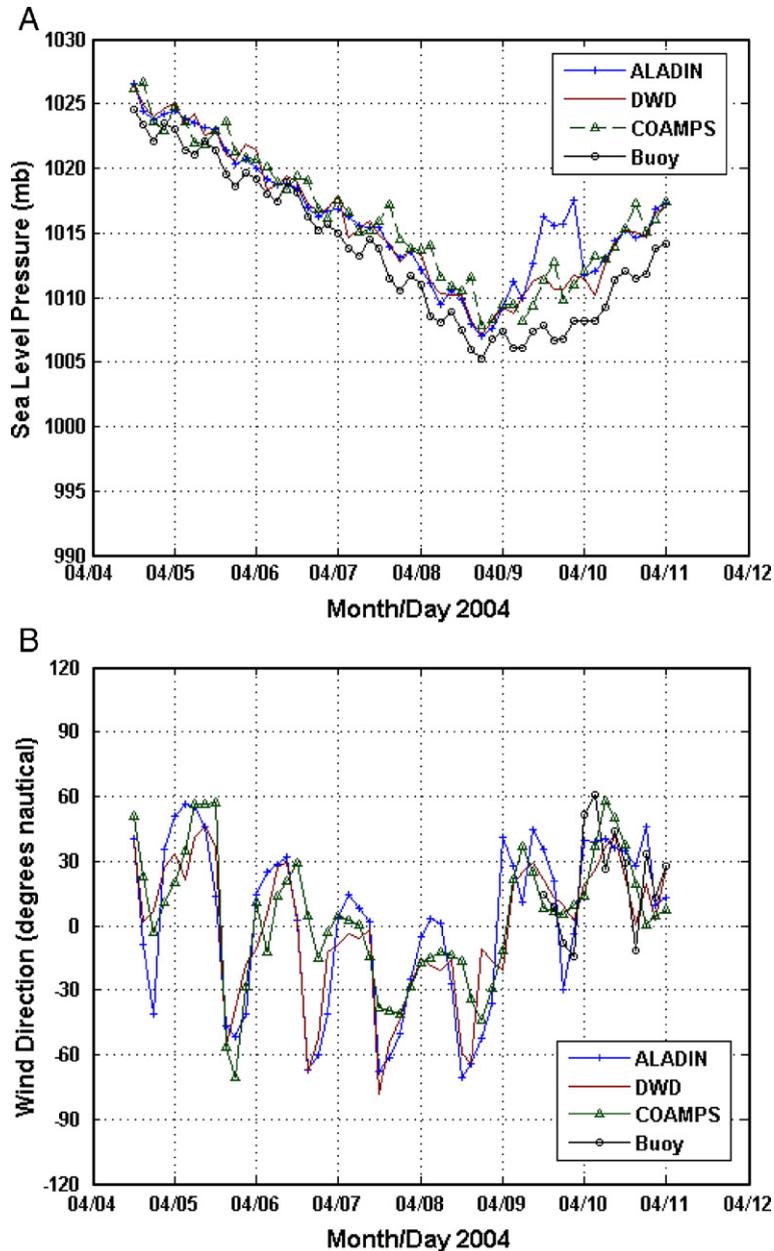
Fig. 6. (A) Sea level pressure (mb) from COAMPS, ALADIN, DWD-LM and Meteo buoy for the period April 4–11; (B) same as a, but for wind direction. Buoy data are missing from April 4–9 (18 GMT); (C) same as a, but for wind magnitude (m/s).
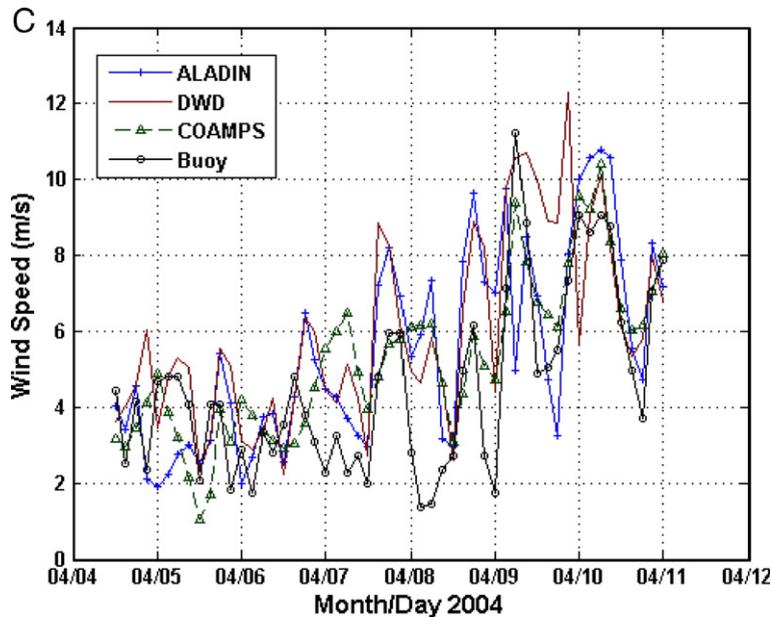
Fig. 6 (*continued*).

wave model in stationary mode. A master module coordinates the two components which are coupled together to simulate wave–current interaction. A communication file acts as the interacting transfer staging point for exchanging data between the two models.

4.2. Domain and bathymetry

Using RGFGRID, a grid-building tool of Delft3D, domains for the WAVE and FLOW modules were established based on the availability of the water depth data and the location of the Pinheiro da Cruz beach. Due to their geographic orientation, both computational grids could be laid conveniently into the Universal Transverse Mercator (UTM) coordinate system. The resolution of the WAVE domain was about 20 m in the X-direction and 40 m in the Y-direction, while that of FLOW varied from 10 to 30 m. On each side of the WAVE domain, the lateral boundaries were placed about 500 m beyond the FLOW lateral boundaries away from the center to keep the wave forcing from introducing spurious forcing gradients at those boundaries. Thus the length of the FLOW domain was about 2.5 km along the shore while the WAVE domain turned out to be about 3.5 km. The width from the shore of both domains was about 1 km. Fig. 4 depicts the relationship between the two grids. The outer box is the WAVE grid and the FLOW grid is represented by the coverage of bathymetry.

Water depths taken from the SHOALS LIDAR data collected during the Linked Seas 2000 exercise were used as the initial depths for Delft3D. Using the Delft3D tool called QUICKIN for applying bathymetry to the grid, the sampled water depths were interpolated to the WAVE and FLOW grids. The sample depths were dense enough that a simple grid cell averaging routine in QUICKIN was sufficient to populate all the grid points with some minor fill in. Fig. 4 depicts the water depths used for the FLOW domain. Within about 500 m of both lateral boundaries of the FLOW domain are artificially extended values to allow for a smooth transition from the boundaries. The purpose of this smooth transition is to prevent the lateral boundaries from generating artificial secondary flows that may enter the domain (Roelvink and Walstra, 2004). Values not shown for the WAVE domain are also extended for the same reason.

Initially, all the grid points in the FLOW and WAVE grids were equidistant and perfectly rectilinear. To enhance computational performance, the grid points for the FLOW domain were later thinned out at points more distant from the area of interest.

In addition to accounting for a two-dimensional domain of variable water depths, Delft3D can incorporate other two-dimensional inhomogeneous boundary conditions such as winds, water levels and wave spectra. In this case, the domain was deemed small enough to assume a uniform wind and water level. However, at the boundaries there were spatially varying wave conditions which were delivered in the form of spectra data output from the SWAN innermost nest (Grid C) in DIOPS, giving six points for each lateral side and ten points on

the seaward side. This level of detail may be important particularly when bars are not present as the variable wave energy may still produce rips.

All the details associated with the domain grids, water depths, the numerical and physical parameters and outputs were set-up ahead of time using the Delft3D graphical user interface. Except for some small adjustments in the numerical behavior, no changes were needed during the exercise. In an operational context, updated bathymetry can be incorporated into the models without interfering with the normal course of operations.
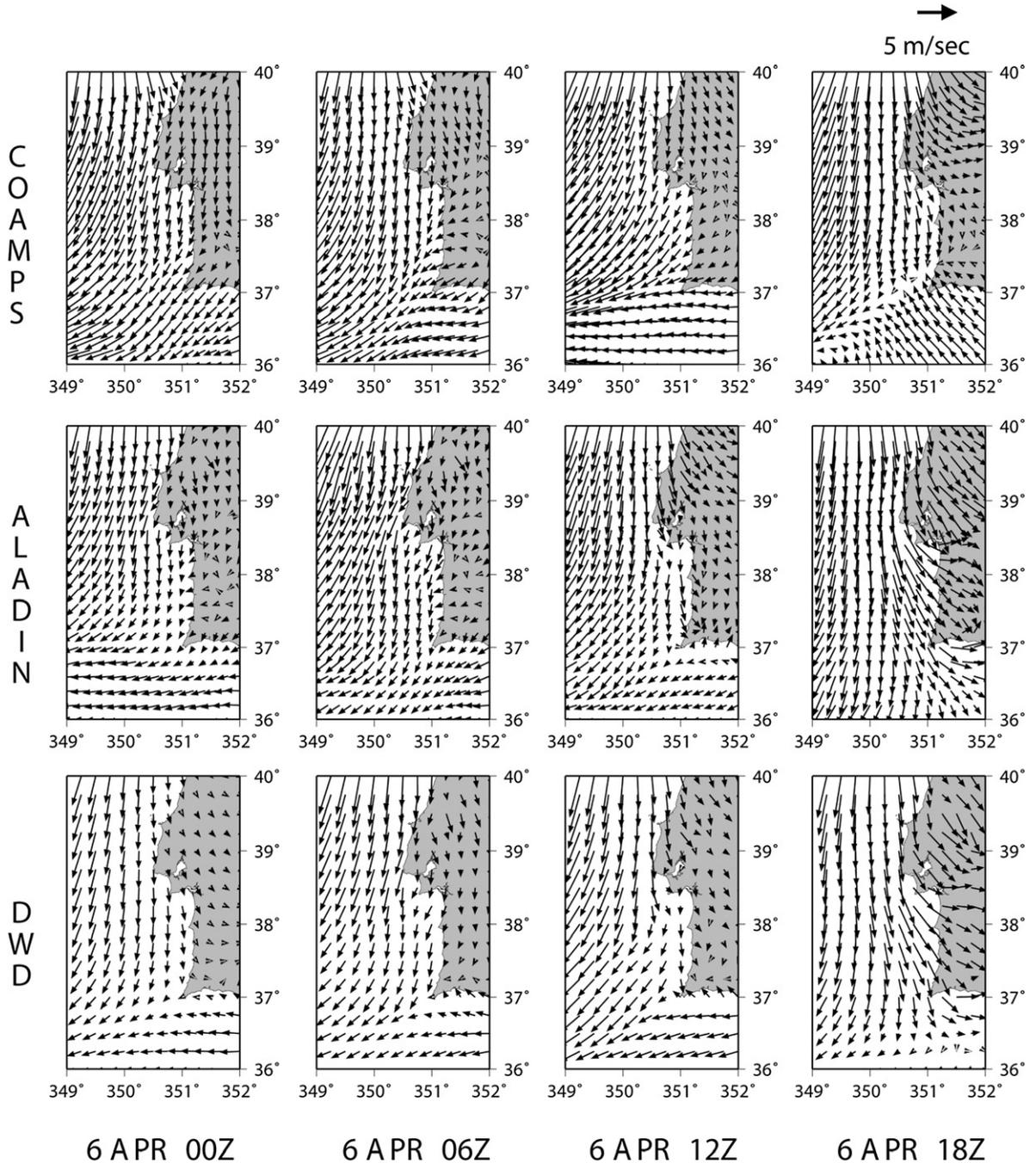
Fig. 7. 10-m winds from (a) COAMPS, (b) ALADIN and (c) DWD-LM on April 6 at 0, 6, 12 and 18 GMT. Data are plotted at 0.2° intervals.

Table 2
Meteorological model specifics

	LONGW	LONGE	LATS	LATN	RES	Output frequency (h)
Model						
ALADIN	349	352	36	40	0.1°	6
DWD-LM	345	354	34	42	0.05°	3
COAMPS	345	40	29	59	0.2°	3

4.3. MREA04 nearshore forecast operations

Each day DIOPS produced a 48-h forecast starting at 00 GMT, resulting in a set of files with spectra, winds and water levels retained for Delft3D. Utilities were developed to extract the needed information from those files and to incorporate that information into the Delft3D configuration files, all in an automated fashion.

Initially, due to some time dependence limitations in the WAVE module, the run-time strategy was to run individual simulations of WAVE and FLOW for certain points in time. The SWAN model in the WAVE module provided forcing for FLOW which would run for 60 min, the time period considered sufficient to reach equilibrium holding all other conditions such as water level and wind constant. This configuration in effect resulted in stationary conditions, i.e., to a point of equilibrium. In this way, we chose to run Delft3D for every 3 h throughout the forecast period. Coupling to the wave–current interaction was one-way (waves forcing currents).

After the exercise, a time-dependent capability was incorporated into the WAVE module software allowing for model suite execution to be performed in a continuous fashion after a one-time set-up. For a hindcast of the entire period, FLOW ran continuously interrupted only by the hourly run of the WAVE module. This mode allowed for the input of time series of water levels and wind inputs. The WAVE module can interpolate from the spectra input and can keep its continuity using restart files. Two-way coupling to simulate wave–current interaction in a real-time situation is now feasible.

5. Observations and measurements

5.1. Surf zone wave and current measurements

Measurements of waves and currents in the nearshore were collected by deploying three different Nortek Vector acoustic velocimeters in the surf zone (Fig. 5).

These sensors are capable of simultaneously measuring the fluid pressure and three orthogonal components of velocity at a single location. The sensors were equally spaced in the longshore spanning a total length of 100 m. At the time of installation, all sensors were placed at low tide in 1.5 m water depth in the shoreward most trough of the study site. The two southern most sensors (N9 and N6) were connected to a shore-based laboratory by means of a data cable through which power was supplied to the sensors so that two-way communication permitted remote control of the data collection procedure and real-time data telemetry. The raw data were collected at 8 Hz and stored for later processing. Archived data were cleaned as described by Elgar et al. (2001) and reduced to 2 Hz. The northernmost sensor (N4) was developed as part of an autonomous beach monitoring system and data processing occurred in the accompanying underwater package after which the analyzed parameters were transmitted to a home laboratory through Iridium satellite modem. For this sensor, analysis was based on collection of 12 min of 8 Hz data every 2 h.

5.2. Imagery at the beach

An image monitoring system for the surf zone was also deployed as part of the MREA04 experiment. This system contained both a digital camera and color digital video camera. The digital camera was used to collect high-resolution (3.7 M pixel) snapshots of the site and the video camera was used to collect high-frequency (~ 2 Hz) images for a sustained period of time from which a single time exposed image (Lippmann and Holman, 1989) was formed. Both cameras were mounted on a common pan-tilt device and images spanning the entire beach were collected by progressively repositioning the field of view of the cameras from south to north. The cameras were mounted on the bluff behind the beach at an altitude of 22 m and a distance of approximately 95 m behind the shoreline (Fig. 5). The monitoring system was programmed to collect a complete series of four images from each camera three times a day (morning, noon and evening). The time-averaged images were processed onboard the system central control unit and the final images were transmitted remotely using FTP protocol over a V-Sat Internet connection. Using techniques (Holland et al., 1997) which were provided by the ARGUS program (Holman et al., 1993; http://cil-www.coas.oregonstate.edu:8080/), the images were subsequently rectified and merged to form a single view of the study site (for examples, see Figs. 5 and 13).

6. Results and analysis

6.1. Meteorological models versus Meteo buoy

To gain a better understanding of the deepwater wave predictions (next section) that impact the nearshore models, we assess the performance of the three meteorological models. During MREA04, an Aanderaa Instruments Coastal Monitoring Buoy 3280 (hereafter referred to as the Meteo buoy) was deployed west-southwest of Pinheiro da Cruz at a 120-m water depth. The compact data buoy is designed for use in coastal waters, ports and nearshore platforms. This buoy configuration measured wind speed (2.5-m height), wind direction, sea level pressure, wave height, air temperature and water temperature. Fig. 2 depicts the location of the Meteo buoy. The buoy data were not assimilated into any of the meteorological models. The processed buoy data
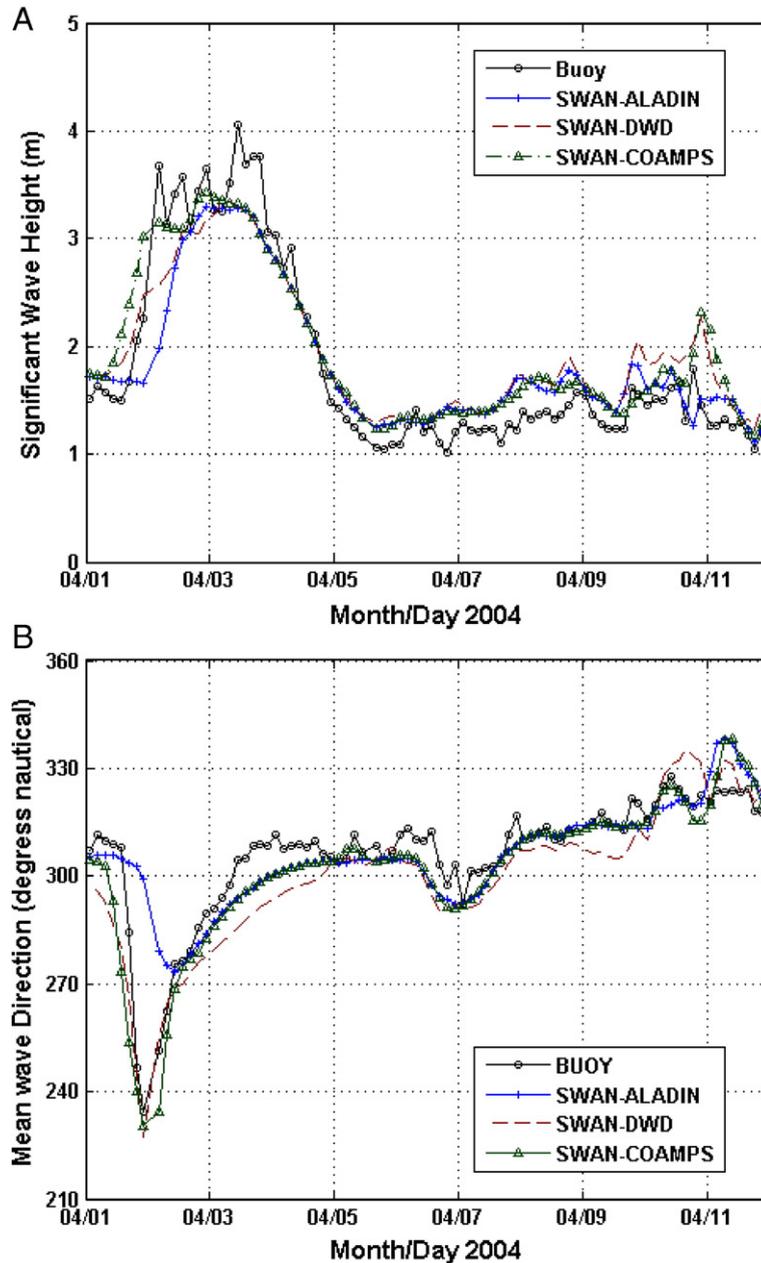
Fig. 8. (A) Significant wave height (meters) during the period March 31–April 11 (00 GMT) at the Sines buoy location versus SWAN forced with ALADIN, DWD-LM and COAMPS 10-m winds; (B) same as a, but for mean wave direction (°); (C) same as a, but for peak wave period (seconds).
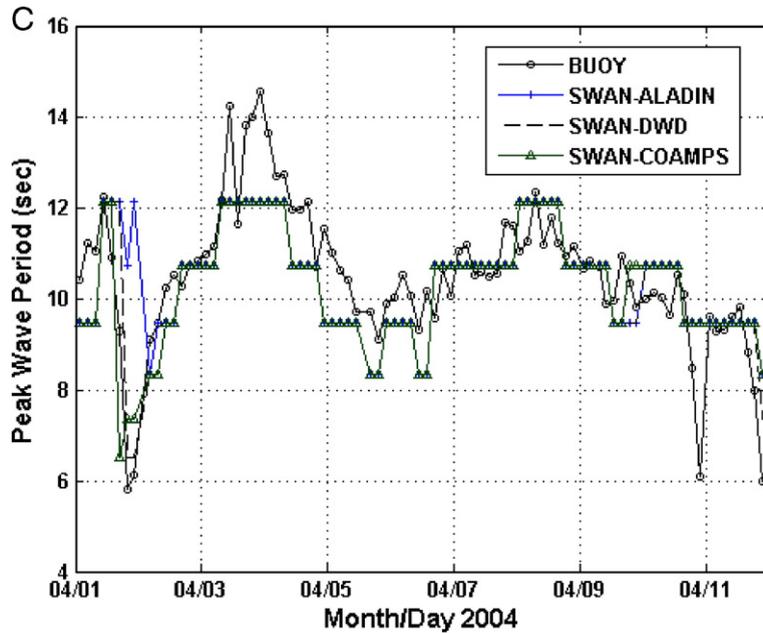
Fig. 8 (*continued*).

were available at approximate one-hour intervals. In the following section, three-hourly buoy data are compared against modeled data at that same interval.

Fig. 6A shows a comparison of sea level pressure from all three meteorological models versus the Meteo buoy during the period of April 4–11, 2004. There is very good agreement among all the meteorological models with the exception of higher values from ALADIN on April 9. Overall, the models compare well against the buoy, although the buoy consistently reports lower values by about two to three millibars during the period.

The wind directions during this period are displayed in Fig. 6B. The models are in general agreement throughout the period, although COAMPS does not reflect the shift from offshore to onshore flow as well as the ALADIN and DWD-LM models. This could be attributed to the frequency of COAMPS output which was available at six-hourly intervals compared to three-hourly for the other models in addition to the relatively coarse 27-km horizontal grid resolution. A diurnal cycle

is evident throughout the period as heating over land generates a late afternoon sea breeze. The pattern reverses during the evening hours. Unfortunately, the wind direction sensor aboard the Meteo buoy was not functioning properly until the afternoon of April 9. During the very short period of good data, there is very good agreement between models and observation.

The Meteo buoy wind speeds were adjusted from 2.5 to 10 m using the simple relationship from Hsu et al. (1994)

$$u_2 = u_1(z_2/z_1)^P, \tag{1}$$

where u_2 denotes the wind speed at the reference height (2.5 m), z_2 and u_1 represents the wind speed measured at height z_1 (10 m). The exponent, P, is set to 0.11 based on an empirical relationship for typical ocean conditions.

Fig. 6C presents a comparison of modeled 10-m wind speeds versus the adjusted 10-m wind speed

Table 3
SWAN wave model statistics at Sines, Portugal, forced with different meteorological models

	ALADIN				DWD-LM				COAMPS			
	RMS	Correlation	Bias	Scat	RMS	Correlation	Bias	Scat	RMS	Correlation	Bias	Scat
H_s (m)	0.34	0.94	0.59	0.186	0.34	0.96	0.69	0.189	0.32	0.95	0.56	0.177
Direction (°)	11.7	0.72	127.2	0.038	10.08	0.92	−26.96	0.033	8.15	0.94	−45.21	0.027
T_p (s)	1.35	0.55	6.28	0.128	1.05	0.76	3.66	0.100	1.09	0.74	3.98	0.103
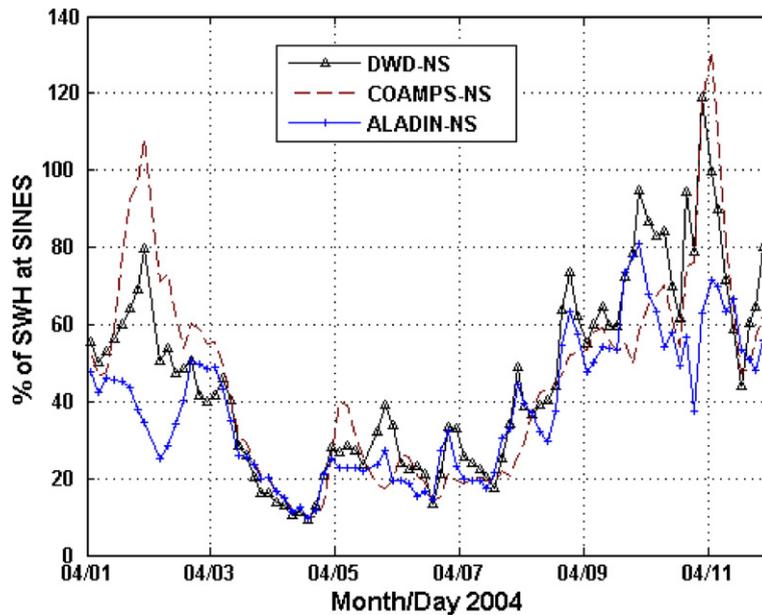
Fig. 9. Ratio of significant wave heights for simulations performed with three different wind models without spectra applied on the model boundary divided by the observed wave height at the Sines buoy. Low percentages indicate that swell energy dominates while high values suggest that local wind generation is the primary mechanism for wave growth.

observed at the Meteo buoy. Overall, the observed wind speeds are lower than modeled by more than 2.0 m/s during this period. We hypothesize that an over-prediction in wind speed by the numerical models may be partially responsible for the higher wave heights (see next section) indicated by SWAN at this location.

A comparison of 10-m winds for the region bounded from 36 to 40°N and 11 to 8°W for April 6 is shown in Fig. 7. Data are plotted on a 0.2° grid to account for the differing model resolutions (DWD-LM had the highest resolution at 0.05°, while COAMPS had the lowest resolution at 0.2°). While all three models indicate a switch from north to north–northeasterly flow to north–northwesterly flow by 18 GMT near the Meteo buoy, the magnitude is weakest from COAMPS.

6.2. SWAN versus SINES buoy

During MREA04, SWAN predictions were made daily aboard the NRV Alliance for the period April 2–10, 2004. Wind forcing consisted of the DWD-LM meteorological model, covering the same domain as the SWAN host grid, with a resolution of 0.05°. In this study, we performed three hindcasts using the following meteorological atmospheric models: (1) DWD-LM, (2) ALADIN and (3) COAMPS-Europe. Table 2 provides information about these models including horizontal and temporal resolution of forecast fields.

A directional deepwater "WAVEC" buoy moored at a depth of 97 m near Sines, Portugal (denoted as a star in Fig. 2) was used to evaluate the performance of SWAN using the three meteorological models described earlier. Fig. 8A–C show a comparison of significant wave height, mean wave direction and peak wave period during the period March 31–April 11, 2004. Buoy data were available at four-hourly intervals. A major storm event occurred during April 1–3 with wave heights at the buoy exceeding 4.0 m on April 3. An intense storm located near 46°N, 13°W on April 1 produced swells that reached this area a few days later.

Table 3 summarizes the comparisons between SWAN (host grid) at the Sines buoy forced with the three meteorological models. However, since the directional wave spectra provided by WAVEWATCH III is forced with COAMPS, it was not possible to determine if those other models (e.g., ALADIN) would have produced significantly different results. Significant wave height RMS error statistics show that all three models performed similarly with a slight edge given to COAMPS whose RMSE ranged between 32 and 34 cm with correlation coefficients falling between 0.94 and 0.96. Scatter indices for all three test cases were consistently in the 18- to 19-cm range. The scatter index is defined as RMSE divided by mean of the observations.

Fig. 8B shows that the hindcasts performed with ALADIN missed the turning of the waves from

northwesterly to southwesterly on April 1. The RMS wave direction errors were near 10°, with COAMPS displaying the lowest error (8.1°) and highest correlation ($r=0.94$). All three models under-predicted the 14-s peak periods shown in Fig. 8C on April 3 and over-predicted the peak period on April 10. The DWD-LM

and COAMPS showed RMS errors at 1.1 s, with the highest correlation ($r=0.76$) with the DWD-LM. Overall, all three meteorological models with different resolutions and physics produced similar results when forcing SWAN. Scatter indexes for peak period and wave direction were small for all three test cases.
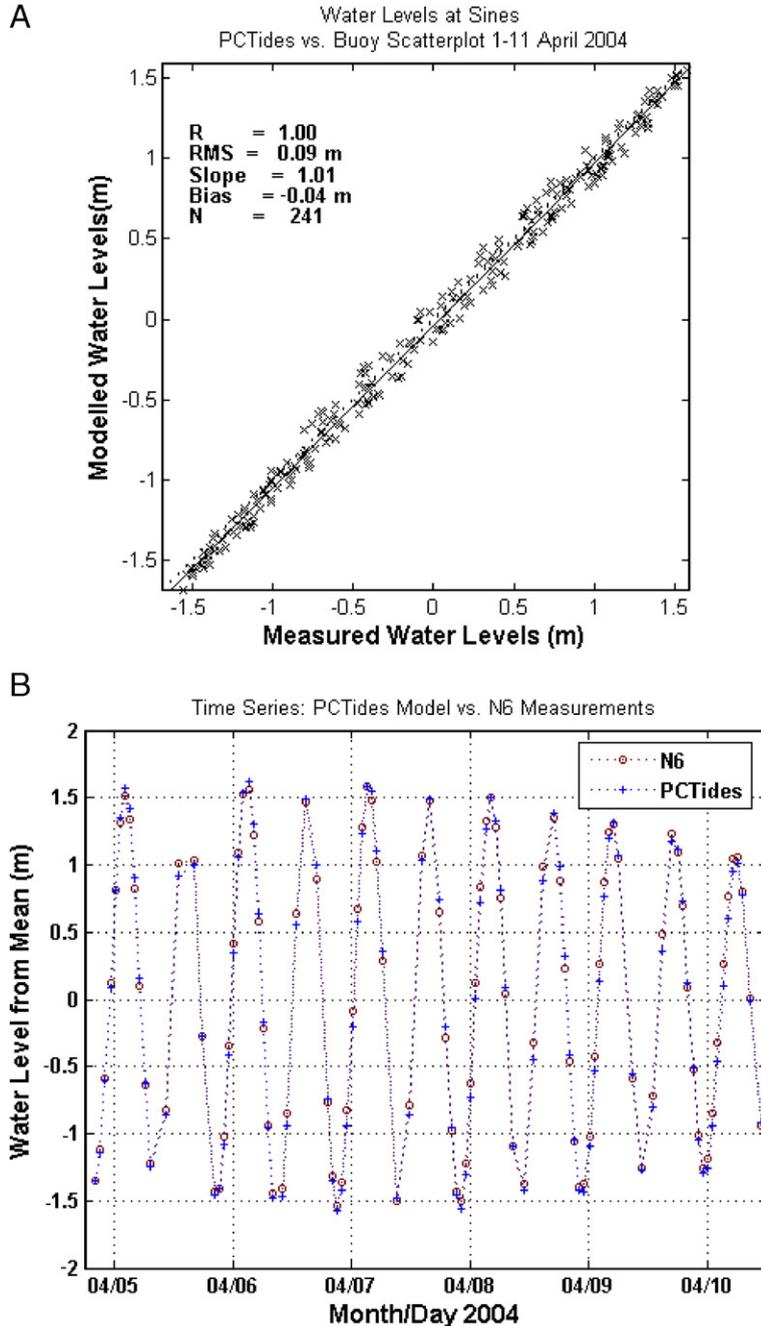
Fig. 10. (A) PCTides water levels (meters) versus data collected by FS Borda; (B) PCTides water levels (meters) versus data collected from N6 near Pinheiro da Cruz; (C) Scatter plot of PCTides water levels versus N6 data.
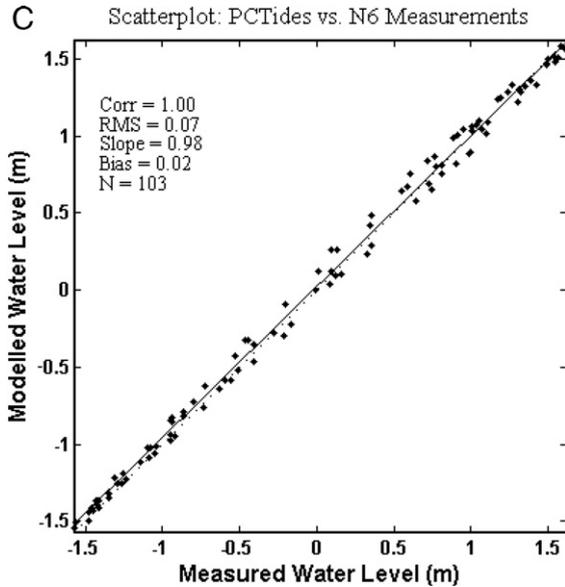
Fig. 10 (*continued*).

The hindcast experiments described earlier were all
driven with WAVEWATCH III wave spectra forced with
COAMPS-Europe wind fields. We did not have wind
forcing available for the Atlantic Basin to examine the
performance of WAVEWATCH III with the other
meteorological models or their operational counterparts
(e.g., DWD global model). To investigate the effect of
offshore boundary conditions on these hindcasts, three
additional experiments were performed in which
boundary forcing was not applied to the SWAN host
grid. Each experiment was forced with wind only from
the three meteorological models described earlier. Fig. 9
depicts the percentage of the significant wave height
(with no boundary forcing) divided by the observed
wave height observed at the Sines buoy location. A
value of 100% indicates wind-generated waves are
generated without regard to swell generated outside of
the model domain. Lower values (e.g., 10–50%) imply
that the propagation of swell events is not represented by
the exclusion of boundary forcing. All three wind models
produced similar SWAN wave heights during the period
of April 3–8 with differences between all three tests at
less than 20%. After that period, COAMPS and DWD-
LM winds produced wave heights 10–30% higher than
observed on April 9, while ALADIN wave heights show
much better agreement with observations. To summarize:
when energy (e.g., from WAVEWATCH III) from outside
the SWAN host domain was dominant, wave heights for
all three hindcasts were similar. However, when wind
forcing was dominant (e.g., on April 2 and 10), sig-

nificant differences among the hindcasts performed with
the three meteorological models was evident. Further
review into this topic could address how to improve
operational wave forecasts where local wind generation is
dominant.

6.3. SWAN versus Meteo buoy

The Meteo buoy was damaged during a previous
exercise, laying doubt about the trustworthiness of the
wave data. The wave periods and wave heights were not
realistic compared to buoy observations at Sines and
nearshore data collected near Pinheiro da Cruz.
Therefore, we do not show any comparisons at this
location. However, we feel that SWAN tended to over-
predict wave heights in this general area possibly due to
sheltering effects from the land features north of this
area for which we did not account.

6.4. PCTides versus gauge and N6

Comparison of PCTides water levels from two
different data sources indicate that PCTides provided
very good agreement in amplitude and phase during the
MREA04 Trial. Fig. 10A depicts a comparison of water
level from PCTides versus data collected by the gauge
data collected at Sines. PCTides demonstrates skill in
the amplitude and phase; the correlation coefficient for
this comparison is 1.0 with an RMSE of 9 cm.
Fig. 10B and C show a comparison of water levels at
Pinheiro da Cruz from PCTides versus a Nortek current
meter deployed during MREA04. The mean water depth
from the period of record from the Nortek6 (hence
referred to as N6, see Fig. 5 for location) was subtracted
from the measured water depth to determine the water
level. Data were recorded at irregular intervals (approx-
imately every 60 or 120 min); PCTides water levels
were interpolated temporally to the N6 observation
times. The data show excellent agreement with an
RMSE in amplitude of 8 cm, phase errors less than
15 min and a correlation coefficient just under 1.0.

Table 4
Statistics for Delft3D versus N6 for period April 4–11, 2004

	No. of observations	RMS	Correlation	Bias	SI
H_s (m)	103	0.21	0.70	0.14	0.33
Direction (°)	103	4.50	0.70	−1.85	0.02
U-current (m/s)	103	0.08	0.53	0.04	−1.20
V-current (m/s)	103	0.14	0.66	−0.04	−1.35
Water level (m)	103	0.07	1.00	0.02	–

6.5. Delft3D versus N6

As discussed earlier, Delft3D was originally run in a stepwise fashion, essentially in stationary mode for instances in time at three-hour increments. Later, the configuration was adjusted to allow for a ten-day hindcast in continuous mode and included an improved configuration and an updated bathymetry based on newly available information. By the end of the exercise, data from all the in situ measurements were tabulated and made available for comparison. Data from the center gage labeled N6 were compared to model output of currents, wave heights and wave direction at the corresponding grid point of the model domain. Analysis
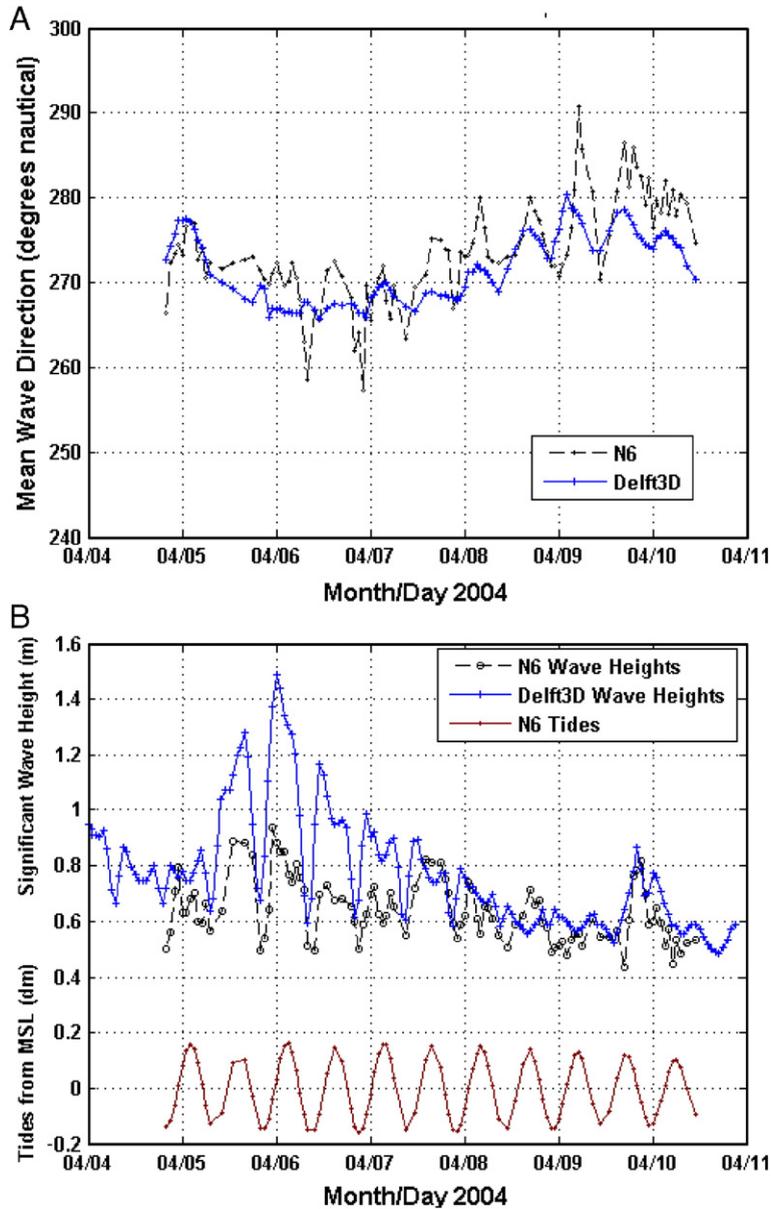
Fig. 11. (A) Time series of Delft3D model output and N6 measurements of wave direction. (B) Time series of Delft3D model output and N6 measurements of significant wave height. Tides from the same measurement device were added for comparison. (C) Scatter plot comparing model output and N6 measurements of mean wave direction. (D) Scatter plot comparing model output and N6 measurements of significant wave height. (E) Time series of Delft3D wave height with and without winds at N6.
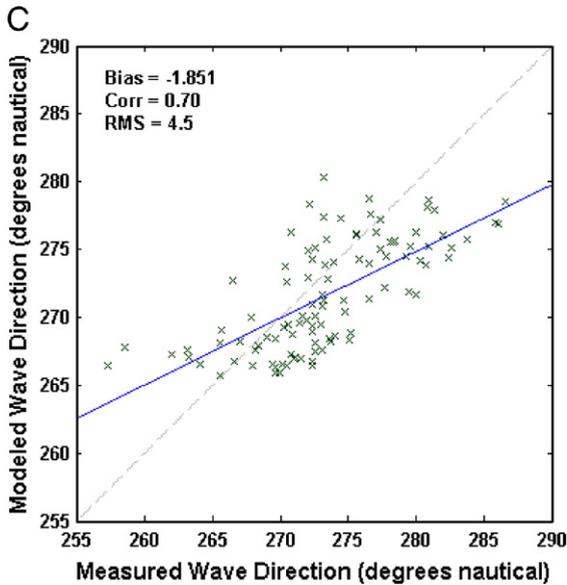
Fig. 11 (*continued*).

of Delft3D output to locations N4 and N9 indicated little model skill. Uncertainties in the nearshore bathymetry at these particular locations are attributed to this discrepancy. Table 4 presents a summary of statistics for wave heights, wave direction, cross-shore and longshore currents and water levels from the model versus data collected at N6.

Fig. 11A depicts the time series of wave direction for both Delft3D and N6, whose comparison shows good agreement. With the beach almost facing west, the incoming wave angle centered around 270° implies that rip currents will generally occur. It is expected that wave direction would refract to almost perpendicular to the shore by the time wave trains reach the surf zone. Still, even a small inclination of wave direction could effect local circulations significantly.

In Fig. 11B the time series of significant wave height from the model and N6 is plotted. In addition, the water levels are plotted to help point out that during periods of low tide when the waves are dramatically affected by the bar, both model output and N6 measurements show low wave heights as would be expected. The bar causes the waves to lose much of their energy due to breaking. However, during high tide, waves propagate over the bar and break closer to the coast. Fig. 11D depicts a scatter plot comparing the modeled significant wave height to the N6 gage including statistics, which show a considerable positive bias. Many of those points contributing to this bias occurred during the period April 5–7, in

which time the boundary inputs were reaching 1 m, so that the model output for wave height at high tide was substantially higher than the measurements. The migrating bar certainly contributed to the discrepancy. This discrepancy may be also due to the fact that the boundary conditions result from a running string of interdependent models rather than from a source ground-truth data, which is expected. For every step taken to model the ocean waves, another factor of inaccuracy is introduced. The original source of the error may have been in the regional SWAN model due to its weakness in handling the sheltering from the energy by the land features to the north.

It is useful to examine the relative importance of wind waves against swells at N6 buoy. If the swell energy is dominant for the whole study period, then the importance of using a good local wind wave model is reduced. The comparison of Delft3D results between with- and without-wind inputs is presented in Fig. 11E. Wind waves are found to be increasingly important after April 8, when the input swell direction veers further to the north. This is certainly due to the effect of headland blocking (see the land features in Fig. 1). The increased blocking is consistent with the wave angle plot as shown in Fig. 8B. The inaccuracy (i.e., wave angle and directional spreading) of WAVEWATCH III spectra could have also significantly affected the Delft3D results. There is no measured offshore wave data for verification. However, the agreement of SWAN output at the Sines buoy in the south (as shown in Fig. 8) tends to indicate that WAVEWATCH III provided good input spectra.

Comparisons of the components of currents along the shore and across the shore were plotted separately in a time series and showed some agreement as depicted in Fig. 12A–B, respectively. At high tide, very little current is induced due to wave breaking at the bar and the model demonstrates that as expected. At low tide, the model output indicates there should be an induced current in both the cross-shore and longshore directions. The longshore component compared well with a correlation of 0.66, but the cross-shore currents compared less favorably, where the correlation was 0.53. The current from the Delft3D output is depth averaged, but the measurements are at a particular depth. Since longshore current is relatively homogeneous over depth, depth average current reasonably represents the reality. On the other hand, the cross-shore current consists of significant undertow. This makes direct comparisons somewhat unrealistic since the variability of the current field with depth is substantial, even reversing direction with depth.
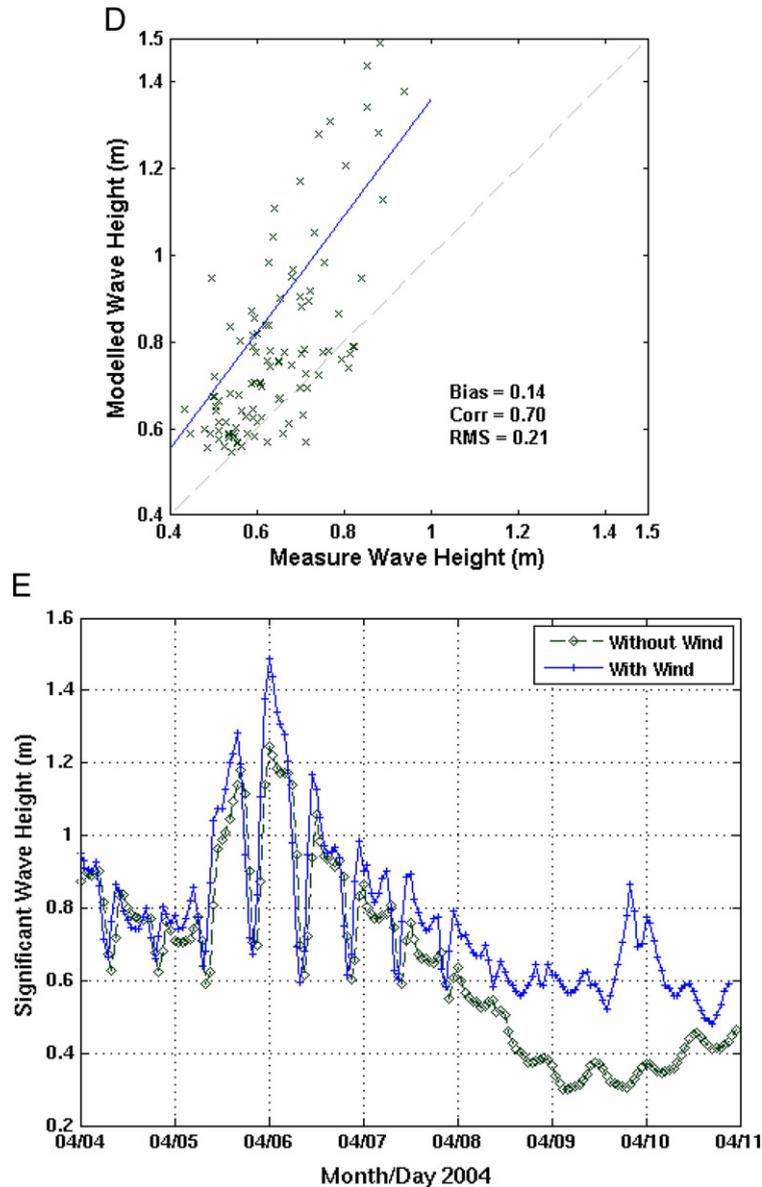
Fig. 11 (*continued*).

6.6. Qualitative evaluation of Delft3D verses video imagery

Comparisons between model and measurements at a single point give only a limited indication of the model performance and observations. For a more complete, observable picture of the area of interest, video imagery was taken at the beach site for which snapshots and time-lapse averaged imagery were generated. This imagery was processed into geographically rectified images for ease of comparison to data also geograph- ically referenced. Fig. 13 shows a time-averaged image taken on about April 7 at 10 GMT with Delft3D model output points showing vectors of current superimposed over the image. On the image the lighter shaded regions associated with whitecaps and bubbles are indicative of breaking waves and from this one can infer the presence and effect of the bar. At intervals along the bar front, breaks in the bar can be inferred where less wave breaking occurred and more cross-shore, seaward cur- rent should flow. The comparison suggests qualitatively some agreement between the Delft3D currents and the
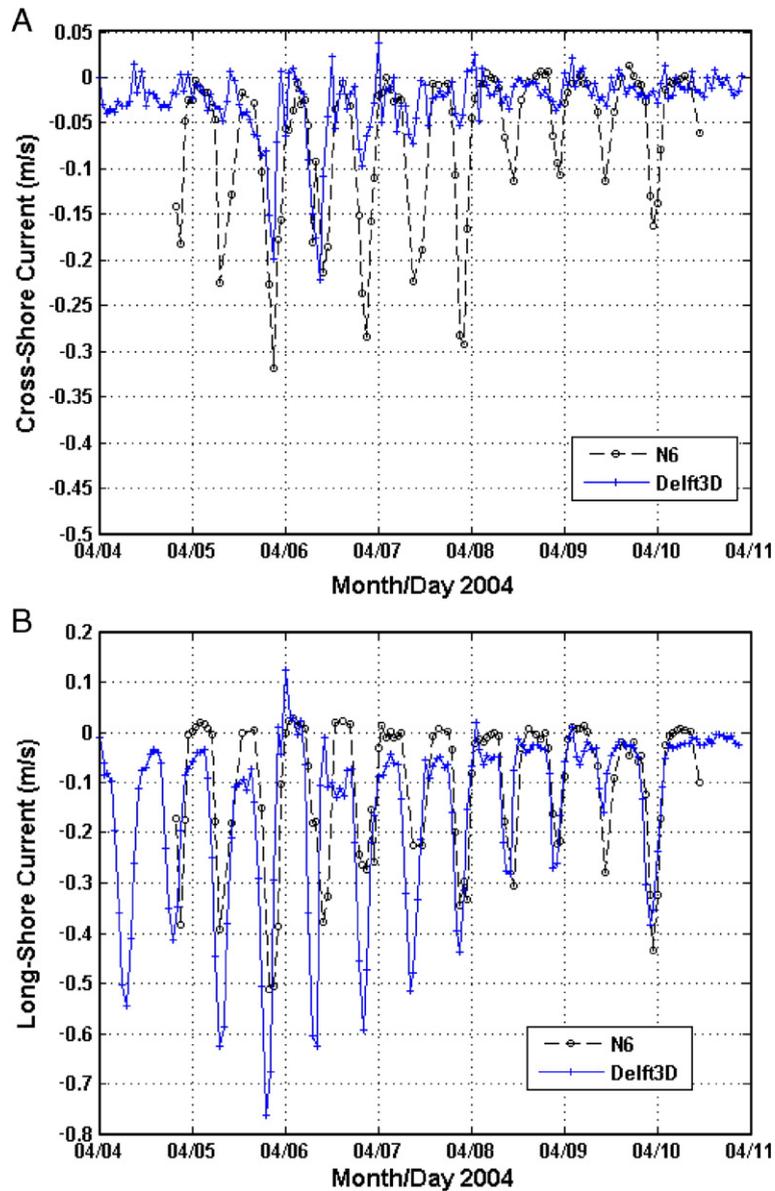
Fig. 12. (A) Time series of Delft3D model output and N6 measurements of cross-shore current. (B) Time series of Delft3D model output and N6 measurements of longshore current.

inferred locations of the flow. Since the bathymetry measurements were not recent, effects of the bar are expected to be different.

7. Summary

A real-time wave, tide and nearshore prediction system can provide valuable information for planning operations by describing nearshore characteristics in littoral areas that include the location and generation of rip currents and surf conditions. The system described

in this paper addresses a nested modeling approach with a series of telescoping models acquiring increasing resolution and smaller geographical coverage as one approaches the desired beach location(s). In this study, a multi-nested wave model is used to provide boundary conditions to the nearshore Delft3D modeling system. Reasonable bathymetry was available for deeper water (greater than 15 m water depth); however, we utilized LIDAR bathymetry collected 4 years earlier for the nearshore modeling. Uncertainties in the nearshore bathymetry due to numerous
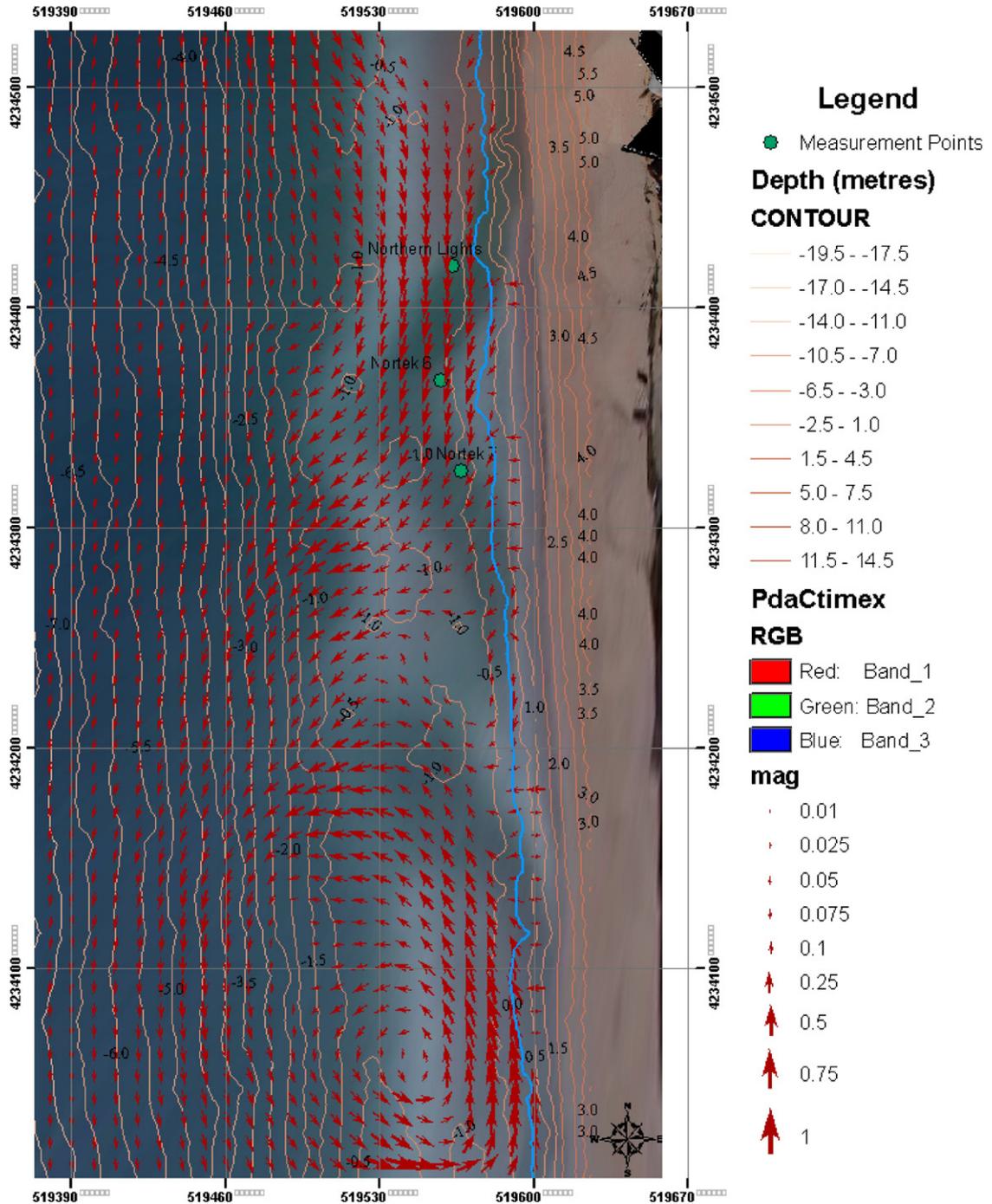
Fig. 13. Time-lapsed imagery with Delft3D output as an overlay. Red arrows depict the magnitude and direction of the current. The coordinate system is in UTM.

storm events, causing the movement of a prominent offshore bar made it difficult to expect predictive skill in this environment.

The PCTides tidal model performed very well in this study as demonstrated with comparisons to measurements with a shallow-water instrument and tide gauge

data at Sines. The accurate water levels were provided to the Delft3D modules to adjust local bathymetry due to tides.

Reasonable comparisons were obtained when comparing SWAN wave height, period and direction when forced by any of the three meteorological models addressed in this study to the Sines wave buoy, located about 45 km south–southwest of the beach experiment area. Improved skill is expected with meteorological models run at higher resolutions to properly resolve mesoscale features including land/sea breezes and orographic effects. These results indicate that the atmospheric models are capable of providing sufficient wind inputs into nearshore wave models.

A nearshore Meteo buoy provided a glimpse of the accuracy of the meteorological models used in this study; however, uncertainties from the wave height sensor make it challenging to adequately assess the skill in SWAN at this location. Future efforts should utilize a network of nearshore buoys for a means of forcing the nearshore modeling system (e.g., buoy directional wave spectra) to evaluate its predictive skill.

The results from Delft3D were mixed and illustrate the need for more accurate input information. One factor that might have contributed to inaccuracies of the model results was the uncertainty of the spectral boundary conditions from WAVEWATCH III which could not be precisely evaluated due to lack of ground truth data right at the boundaries. Another factor was that Delft3D nearshore waves and currents are certainly strongly affected by the migrating sand bars which were not updated due to lack of data. Though the results gave fair indications of the overall surf conditions, more work is needed to improve on the operation of Delft3D to provide more accurate results. We anticipate future improvements towards the collection of more accurate, up-to-date nearshore depth information.

Acknowledgments

References

Allard, R.A., Brooking, M., Dykes, J.D., Miles, K., 2000. Providing operational wave/surf support during NATO Exercise Linked Seas 2000. Proc. 4th International Workshop on Wave Hindcasting and Forecasting, Monterey, California, pp. 85–90.

Allard, R.A., Dykes, J., Kaihatu, J., Wakeham, D., 2005. DIOPS: a PC based wave, tide and surf prediction system. Proc. 6th Conference on Coastal Atmospheric and Oceanic Prediction and Processes, San Diego.

Booij, N., Ris, R.C., Holthuijsen, L.H., 1999. A third-generation wave model for coastal region: 1. Model description and validation. J. Geophys. Res. 104 (C4), 7649–7666.

Doms, G., Schattler, U., 1999. The Nonhydrostatic Limited-Area Model LM (LM-Modell) of DWD. Part 1: Scientific Documentation. Deutscher Wetterdienst (DWD), Offenbach. available at www.cosmo-model.org.

Dykes, J.D., Hsu, Y.L., Kaihatu, J.M., 2003. Application of Delft3D in the nearshore zone. Proc. 5th AMS Coastal Conf., Seattle, Washington, pp. 57–61.

Elgar, S., Raubenheimer, B., Guza, R.T., 2001. Current meter performance in the surf zone. J. Atmos. Ocean. Technol. 18, 1735–1746.

Hodur, R.M., 1997. The Naval Research Laboratory's Coupled Ocean/Atmosphere Mesoscale Prediction System (COAMPS). Mon. Weather Rev. 125, 1414–1430.

Holland, K.T., Holman, R.A., Lippmann, T.C., Stanley, J., Plant, N., 1997. Practical use of video imagery in nearshore oceanographic field studies. IEEE J. Oceanic Eng. 22, 81–92.

Holman, R.A., Sallenger, A.H., Lippman, T.C., Haines, J.W., 1993. The application of video image processing to the study of nearshore processes. Oceanography 6, 78–85.

Hsu, S.A., Meindl, E.A., Gilhousen, D., 1994. Determining the power-law wind-profile exponent under near-neutral stability conditions at sea. J. Appl. Metalwork. 33 (6), 757–765.

Lefevre, F., Lyard, F.H., Le Provost, C., Schrama, E.J.O., 2002. FES99: a global tide finite element solution assimilating tide gauge and altimetric information. J. Atmos. Ocean. Technol. 19, 1345–1356.

Lillycrop, W.J., Irish, J.L., Pope, R.W., West, G.R., 2000. GPS sends in the marines: rapid environmental assessment with LIDAR. GPS World 18–26 (November).

Lippmann, T.C., Holman, R.A., 1989. Quantification of sand bar morphology: a video technique based on wave dissipation. J. Geophys. Res. 94, 995–1011.

Morris, B.J., 2001: Nearshore wave and current dynamics. Ph.D. dissertation, Naval Postgraduate School, Monterey, CA. 89p.

Pires-Silva, A.A., Makararynskyy, O., Monbaliu, J., Ventura-Soares, C., Coelho, E., 2002. WAM/SWAN simulations in an open coast: comparisons with ADCP measurements. Proc. of the 6th Int. Symposium Littoral 2002, pp. 169–173.

Preller, R.H., Posey, P.G., Dawson, G.M., 2002. The operational evaluation of the navy's globally relocatable tide model (PCTides). Proceedings of the Oceans 2002 MTS/IEEE Conference, vol. 2, pp. 847–852.

Reniers, A.J.H.M., Van Dongeren, A.R., Battjes, J.A., Thornton, E.B., 2002. Linear modeling of infragravity waves during Delilah. J. Geophys. Res. 107 (C10), 3137.

Ris, R.C., Booij, N., Holthuijsen, L.H., 1999. A third generation wave model for coastal region, part II: verification. J. Geophys. Res. 104 (C4), 7667–7681.

Roelvink, J.A., 2003. Implementation of Roller Model, Draft Delft3D Manual, Delft Hydraulics Institute.

Roelvink, J.A., Walstra, D.-J., 2004. Keeping it simple by using complex models. The 6th Int. Conf. on Hydroscience and Engineering, May 30–June3, Brisbane, Australia.

Stelling, G.S., Van Kester, J.A.T.M., 1994. On the approximation of horizontal gradients in sigma coordinates for bathymetry with steep bottom slopes. Int. J. Numer. Methods Fluids 18, 915–955.

Tolman, H.L., 2002. User Manual and System Documentation of WAVEWATCH-III Version 2.22. NOAA/NWS /NCEP /MMAB Technical Report, vol. 222.

WL Delft Hydraulics, 2001. User Manual Delft3D-FLOW.